Liquefaction and re-liquefaction potential of the Manu river sand of Tripura, India

Kunjari Mog & Anbazhagan P
Indian Institute of Science, Bangalore, India
Email: mogkunjari@gmail.com

ABSTRACT

During the 3rd January 2017, Tripura earthquake of magnitude (Mw5.7), soil containing appreciate percentage of silts were erupted to the ground surface owing to the liquefaction. Linear, as well as elliptical features sand boils, were observed along the bank of the Manu river, Tripura, India. In the present study, laboratory and field investigations of the same liquefied site soil are reported. In the laboratory, undrained cyclic triaxial tests of sand obtained from the Manu riverbed (from the same liquefied site) is conducted and liquefaction and re-liquefaction potential of the same clean sand results are discussed. The tests were carried out on reconstituted saturated sands at two different relative densities such as 30 % to 70 % under an isotropic effective consolidation pressure of 100 kPa. More, the results of the in-situ liquefaction investigation of the liquefied site are presented using Multichannel Analysis of Surface Wave (MASW) tests in terms of the variation of shear wave velocity with depth.

INTRODUCTION

During earthquakes the ground shaking causes the excess pore water pressure to build up within the soil that in turn reduces the effective stress and thereby reduces the soil strength or stiffness. As a result, gushing of soil-water mixtures to the earth surface, settlement of buildings, failure of foundations, earth dams, landslide, lateral spreading, etc. occurs. This phenomenon of losing strength or stiffness of soils due to the vibration is called liquefaction. Since 1964 after the devastating effects of liquefaction due to the Niigata earthquake in Japan and Alaskan earthquake in USA (Kramer 1996), in the last six decades much progress has been made in understanding the liquefaction phenomenon, identifying the liquefaction related hazards, evaluating the potential of liquefaction in the field as well as in the lab, liquefaction mitigation measures etc. However, damages due to liquefaction are still proving as a leading cause of damages worldwide.

The liquefaction potential of soils influenced by the number of factors includes soil type, stress & strain amplitude, duration of vibrations, the initial state of soils or density, age, percentage of fines presence, hydraulic conditions, etc. Prior to 1980s most of the earlier studies on liquefaction were restricted relatively only to the clean sands as it was believed that fine-grained soils are not susceptible to liquefaction. However, several earthquake case histories in the past indicated that silty soils or sands often containing an appreciable percentage of fines (soil particles smaller than 75 microns) during earthquakes can liquefy as observed in Tottoriken-Seibu earthquake in 2000 (Towhata 2008), Bhuj earthquake in 2001 (Sitharam et al. 2004) to mentioned a few. The liquefaction event in Kanchanbari

due to 3 January 2017 Tripura earthquake (Mog & Anbazhagan 2018, Anbazhagan et al. 2019) brings about the fact that silty sand can liquefy even in moderate magnitude earthquake (Magnitude less than 6.0).

During the 3 January 2017, an earthquake of moment magnitude 5.7 hit the Tripura which caused damages to low rise buildings (mostly damages occurred to unreinforced masonry building) and brought the liquefaction along the bank of the Manu river of Tripura, India. It was for the first time in India where field evidence of liquefaction due to earthquake magnitude of less than 6.0 was documented and reported in the literature (Anbazhagan et al. 2019). In the present study, the results of the laboratory cyclic triaxial and field MASW (Multichannel Analysis of Surface Wave) studies of the same liquefied site is investigated and presented. The probable liquefaction depth due to 3 January 2017 Tripura earthquake is investigated using field MASW testing and reported in the paper. More, laboratory undrained cyclic triaxial tests of clean sand obtained from the Manu riverbed (located from the same liquefied site) is presented for varying relative densities and cyclic stress ratios. The results are presented in terms of the development of excess pore pressure build-up, shear strain accumulation with the number of cycles, stress-strain response, stress-path, and strain-path. The results presented in this paper is a part of the investigations of the ongoing project on "laboratory and field investigations of the liquefied site of Tripura, India".
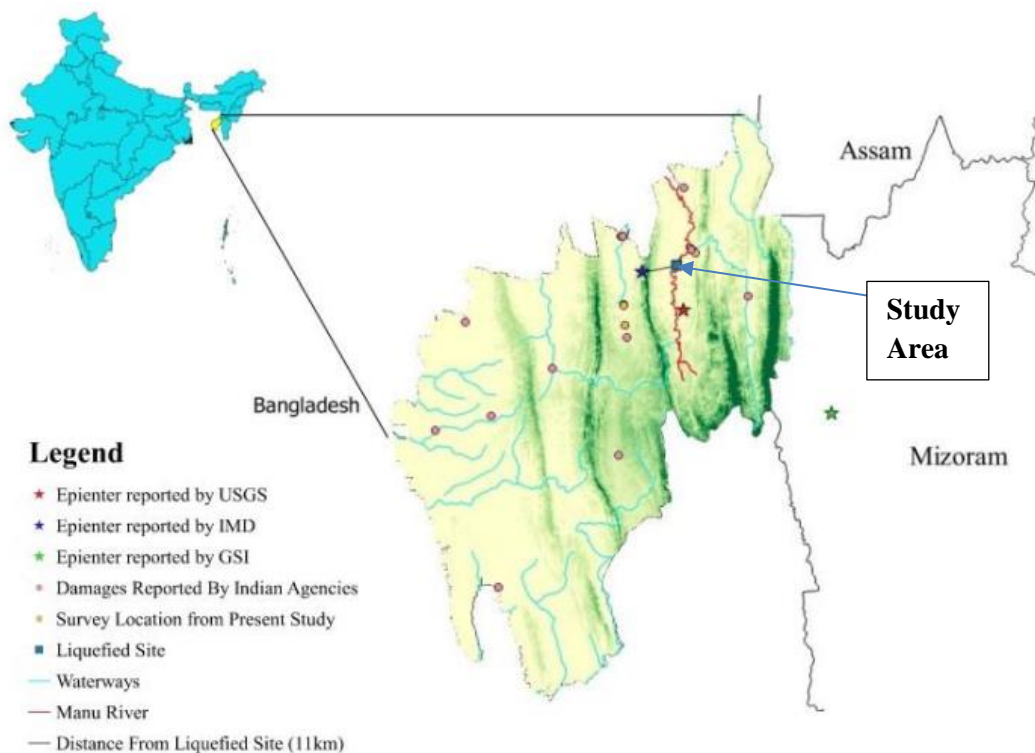
Figure 1. Location of the study area where liquefaction occurred due to 3 January 2017 Tripura Earthquake (reproduced after Anbazhagan et al. 2019)

SITE LOCATION & TEST MATERIALS

Tripura is situated in the north-eastern part of India, situated close to the Himalayan belt. It is identified as a seismically vulnerable state due to the convergent boundary of the Indian plate with the Eurasian plate which is moving at a rate of 4.5 cm per year. The entire state is classified as seismic

zone V as per the Indian seismic code (IS1893:2016) with an anticipated zero period acceleration of 0.36 g. Following the 3 January Tripura earthquake, a team from Indian Institute of Science (IISc) Bangalore visited the liquefaction site and detail studies of the field reconnaissance survey of the geotechnical and structural damage of the earthquake is reported by Anbazhagan et al. (2019). It was reported that the liquefaction site was located at about 11 km away from the epicentre. The site location of the present study area along with the liquefied location caused due to 3 January Tripura earthquake is illustrated in Figure 1.

The first part of this paper presents the field investigations of the liquefaction site using MASW test followed by laboratory liquefaction resistance of the riverbed sand using cyclic triaxial test. The soil material used for the laboratory investigation in this study was collected from the riverbed of the Manu river from the same liquefaction site as shown in Figure 1. The tested soil material is clean fine-grained sand with poorly graded distribution (SP) and with a mean grain size of 0.15 mm. The minimum and maximum dry density of the material is observed to be 1.33 g/cc and 1.68 g/cc respectively. The grain size distribution curve of the tested sand is shown in Figure 2.
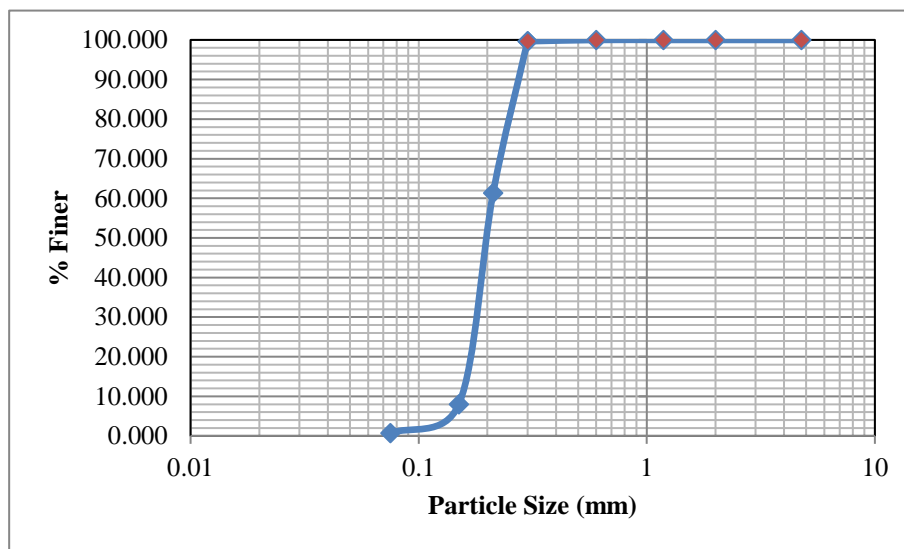
Figure 2: Grain size distribution of the tested Manu river sand

FIELD MASW TEST PROCEDURE

The Multichannel Analysis of Surface Wave (MASW) test which is most popular for geotechnical investigations is used in the present study to measure the shear wave velocity in the in-situ environment at the liquefied site. The MASW test considers the measured ground vibrations as Rayleigh wave (Towhata 2008) which is measured by a set of wave sensors or geophones placed at the ground surface. It generates dispersion curve (Rayleigh wave velocity versus loading frequency) corresponding to the varying wavelength and measures the most probable soil profile. The MASW can be performed in two ways such as by Active test method and passive test method (Tokitmatsu et al. 1992). In the active type method, an artificial source of vibration such as falling weight or mechanical vibrator is used to generate Rayleigh wave of relatively shorter wavelength (measure wave properties at shallower depth). On the contrary, in the passive method, a natural microtremor (ambient noise) of longer wavelength whose source is unknown is used to measure the wave properties at a deeper depth. In the present investigation, the active type method (Chandran & Anbazhagan 2017) is adopted for which a typical test measurement at one of the damaged locations in Tripura is shown in Figure 3.

The MASW test is performed at the liquefaction site by placing 24 geophones at an equal interval of 2 m spacing along the same direction. Each geophone (which act as a receiver of the vibration) of the minimum frequency of 2 Hz is connected to a multichannel recorder and data acquisition system. Once the connection is established, a sledgehammer of 7.8 kg is used to produce the vibrational waves on the ground surface by hitting the metal plate. These vibrational waves which travel from one end to the other end of the geophones are recorded and data is processed. The results of the MASW test obtained from the liquefied site is presented and discussed in the proceeding section.

Figure 3. Multichannel Analysis of Surface Wave (MASW) test at one of the damaged locations in Tripura

LABORATORY SAMPLE PREPARATION & CYCLIC TRIAXIAL TEST PROCEDURE

To investigate the liquefaction and re-liquefaction potential of the Manu riverbed sand collected from the same liquefied site, a cylindrical soil specimen of size 50 mm in diameter and 102 mm in height is prepared and subjected to an undrained cyclic triaxial test. First, the appropriate weight of the air-dried sample is obtained and divided into six equal parts (by weight). Then a latex rubber membrane is fixed at the base pedestal (lower platen) and secured it with three O-rings. Next, a cylindrical split mold of size little larger than the diameter of the triaxial base pedestal is placed around the rubber membrane and membrane is stretched from the top to slide over (folded) the split mold. A porous stone is placed on the base pedestal inside the membrane and constant vacuum of 20 kPa was applied through the bottom of the base pedestal. This application of vacuum helps in removing the entrapped air between the rubber membrane and split mold. Then the split mold is filled with sand in six equal layers. A tamping rod of diameter 31 mm and 250 mm in height (weight of 142 g) is used to compact the soil sample. After achieving the height of about 102 mm, another porous stone and a top cap are placed on the top of the soil specimen. The rubber membrane is then unfolded (which covers the porous stone

and top cap) and sealed it with three O-rings. Finally, split mold is removed while the vacuum application is continued until the application of the cell pressure.

In each case, after preparation of the soil sample, the height and diameter were measured with Vernier caliper and noted down. Once these initial measurements are done, the triaxial cell wall is fixed, placed underneath the loading frame and filled with water. The cell pressure is then applied while simultaneously releasing the vacuum pressure to zero. The CO_2 is allowed to seep through the bottom of the specimen to accelerate the saturation process followed by the water saturation and consolidation. The saturation procedure is explained in detail in the following paragraph.

Table 1. The summary of the B value measurement obtained during the saturation stage.

Time (Approx.)	Drainage Valve	CP (Cell Pressure)	BP (Back Pressure)	Δu (Change in Pore Pressure)	$B = \Delta u / \Delta_{\sigma 3}$
0		40	30	-	-
After 30 minutes	Closed				
		90	40	10	0.20
	Opened				
		90	80	-	-
60 minutes	Closed				
		140	110	30	0.60
	Opened				
		140	130	-	-
90 minutes	Closed				
		190	174	44	0.80
	Opened				
		190	180	-	-
120 minutes	Closed				
		240	225	45	0.90
	Opened				
		240	230	-	-
150 minutes	Closed				
		290	276	46	0.92
	Opened				
		290	280	-	-
180 minutes	Closed				
		340	327	47	0.94
	Opened				
		340	330	-	-
210 minutes	Closed				
		390	377	47	0.94
	Opened				
		390	380	-	-
240 minutes	Closed				
		440	428		0.96
	Opened				
		440	380	-	-
270 minutes	Consolidation	480	380		

To obtain full saturation i.e., B value equals to or greater than 0.96, at first, Cell Pressure (CP) = 40, Back Pressure (BP) = 30 is applied and kept for some time (as presented in Table 1). After 25-30 minutes, CP is increased to 90 kPa (drainage valve is closed), while BP of 30 kPa is held constant. As

confining pressure is applied with an increment of 50 kPa (i.e., 40 kPa to 90 kPa), the pore-water-pressure of the soil specimen increases by Δu (as drainage is prevented). This increase in the pore water pressure is measured & B value is calculated using the expression $B = \Delta u / \Delta \sigma 3$ where, B is referred to Skempton's pore pressure parameter, Δu as the change in pore pressure and Δσ3 as the change in confining pressure.

In the next increment, (drainage valve is opened) CP = 90, BP = 80 is applied and after about 30 minutes, (drainage valve is closed) B value is checked by increasing the CP to 150 and keeping the BP constant (80 kPa). This incremental increase (50 kPa each time) of the CP & BP was then repeated until the required B value is achieved. The difference between CP & BP (effective pressure) is maintained as 10 kPa throughout the saturation process. Also, it should be mentioned here that to obtain the B value greater than 0.95 or to achieve a fully saturated condition, an incremental increase of 50 kPa was maintained.

After the saturation process is completed or achieving the B value greater than 0.95, isotropic consolidation is performed (drainage valve is opened) by increasing the CP while keeping the constant BP. Here, constant BP refers to the pore water pressure reached during the final saturation B-check. The cell pressure is then applied in such a way that the difference between the CP & BP meet the target effective confining pressure, which is 100 kPa in this study. The consolidation is continued for about 20 minutes in each case. Finally, cyclic loading is then applied to the consolidated specimens under the undrained condition. The same procedure is followed (for all the specimens) to conduct the cyclic test at 100 kPa effective confining pressure. The measurement of the Skempton's parameter B obtained for 70% relative density specimen is enumerated in Table 1.

The cyclic test was performed using the GCTS resonant column cum cyclic triaxial instrument and following the specifications of ASTM D5311. The test was conducted on a cylindrical specimen of size 50 mm diameter and 102 mm height under undrained condition by varying Cyclic Stress Ratios (CSR) and relative density. The criteria for initial liquefaction are set such that when the excess pore water pressure reaches equals the effective consolidation pressure or when the double amplitude axial strain amplitude reaches 5 %. After the first initial liquefaction is occurred i.e. when the excess pore water pressures become equals to the 100 kPa effective consolidation pressure, the same soil specimen is reconsolidated (excess pore water pressure is drained out) for about 20 minutes and 2nd liquefaction (re-liquefaction) is conducted. The same procedure is followed to conduct 3rd and 4th liquefaction test on the same soil specimen. It should be mentioned here that the GCTS triaxial system is fully automated and computer-controlled in which experiment can be stopped once the initial liquefaction is achieved. The results for the liquefaction and re-liquefaction potential of the Manu riverbed sand following the same procedure as mentioned above is discussed in the proceeding section.

RESULTS AND DISCUSSION

Field investigation of the liquefied site using MASW

The in-situ Multichannel Analysis of Surface Wave (MASW) test performed at the liquefied site is presented and discussed in this section. Five sets of the active type of MASW test was performed exactly at the same location where liquefaction occurred due to 3 January 2017 Tripura earthquake. The coordinates of the liquefaction site are 24.118°N and longitude 91.991°E (Anbazhagan et al. 2019) located adjacent to the Manu river of Tripura, India. The typical results of the MASW test is presented in terms of the variation of the shear wave velocity versus depth as shown in Figure 4. The results presented here are the average curve of the five sets of MASW tests at the liquefied site.

It can be observed from Figure 4 that the shear wave velocity increases with an increase in depth. However, up to depth of 7 m, lower value of the shear wave velocity is observed. This low patch of shear wave velocities indicates the probable field liquefaction zone from which mixtures of sand-silts were emitted to the ground surface. To investigate further on this the ins-situ cross-hole test and

Standard Penetration Test (SPT) will be conducted in the future at the same liquefied location and will be reported elsewhere.
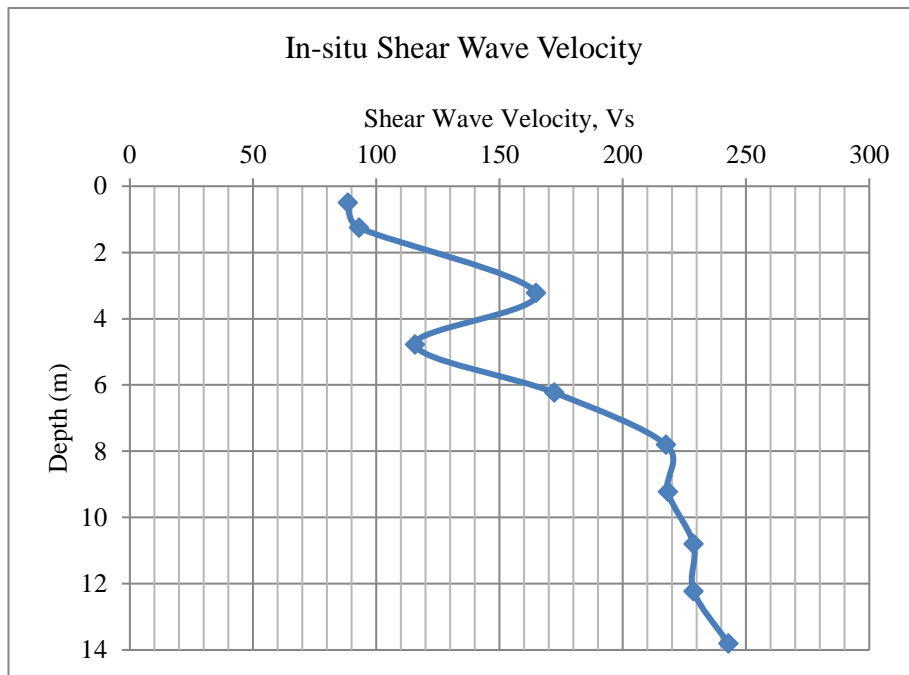
Figure 4. Variation of shear wave velocity with depth at the liquefaction site obtained from MASW test

Liquefaction resistance of loose and dense sand in cyclic triaxial test

Numerous previous reports confirmed that the soil deposits that liquefy in one earthquake can re-liquefy in the next or subsequent earthquakes as also reported by Huang & Miao (2013). Hence, the liquefaction and re-liquefaction potential of the Manu river sand (clean sand) which liquefied during 3 January 2017 is investigated using the cyclic triaxial instrument and results are discussed here. Figures 5 (a – f) and Figures 6 (a – f) indicates the results for liquefaction resistance of the sand; Figures 7 (a – d) indicates the results for re-liquefaction behaviour of the sand.

To investigate the liquefaction resistance of Manu riverbed sand (clean sand) soil specimen prepared at 30 % and 70 % relative density was subjected to different stress ratios and tested under stress-controlled conditions. Figure 5 (a – f) illustrates the data obtained for 30 % relative density specimen on clean sand under undrained cyclic triaxial test corresponding to an effective confining pressure of 100 kPa. Similar to Figures 5 (a – f), Figures 6 (a – f) (on the right) illustrates the undrained cyclic test data for 70 % relative density specimen. The same set of data is replotted for the densely packed specimen to compare the results with the loosely packed specimen.

Figure 5 (a) portrays the time histories of the deviator stress applied on the soil specimen, as a response it can be observed from Figure 5 (b) that axial strain starts to grow rapidly up to 5 % double amplitude strain, though the strain developed is unsymmetrical in this case. However, as can be seen from Figure 6 (b) that the strain developed during the cyclic test is nearly symmetric on both positive and negative sides up to a certain strain level above which (at large strain level) it follows unsymmetrical trend same as that of the loose specimen. Simultaneously, 50 % of excess pore water pressure is reached rapidly in first 2 – 3 cycles for the loose specimen (Figure 5c), but it took about 50 cycles for the dense specimen (Figure 6c). The excess pore water pressure reaches the maximum value at 11 number of successive cycles (Figure 5c) for loose specimen and about 250 cycles for the dense

specimen (Figure 6c). Hence, it is amply clear that the number of cycles required to cause initial liquefaction in case of the dense specimen is much greater than those of loose specimen.
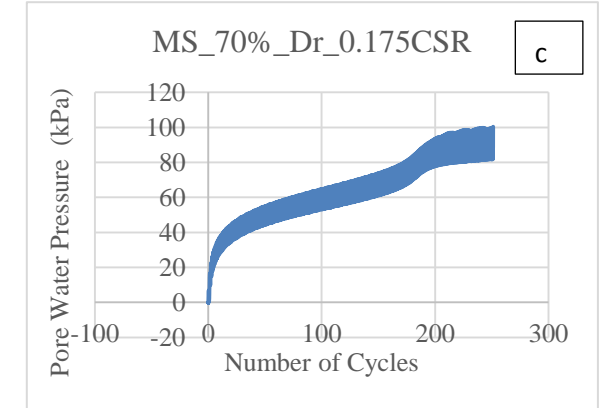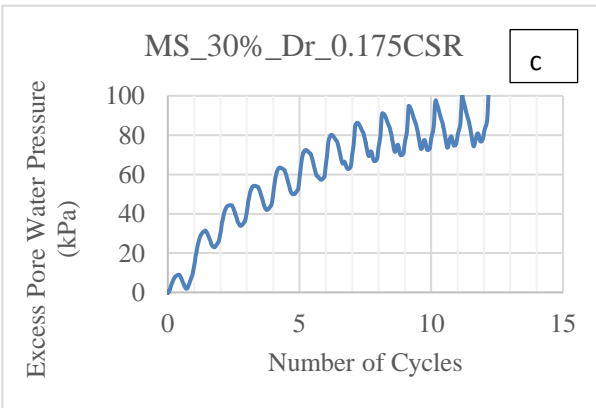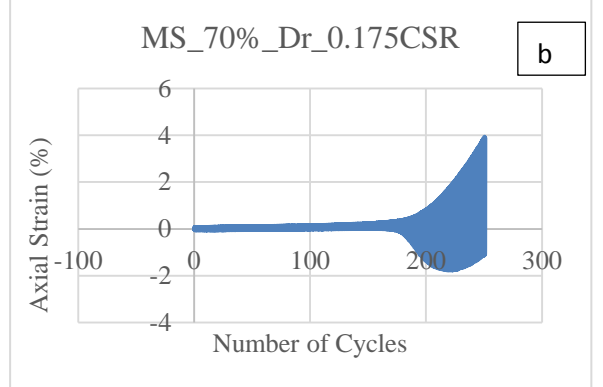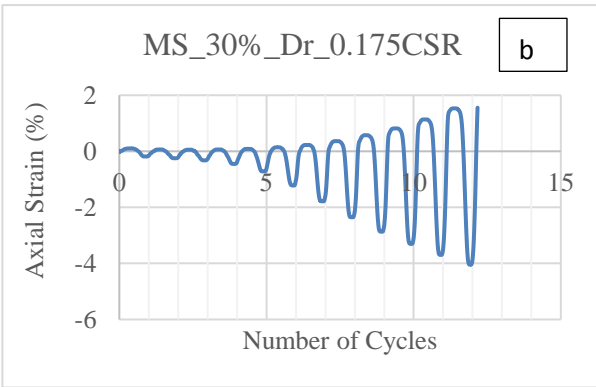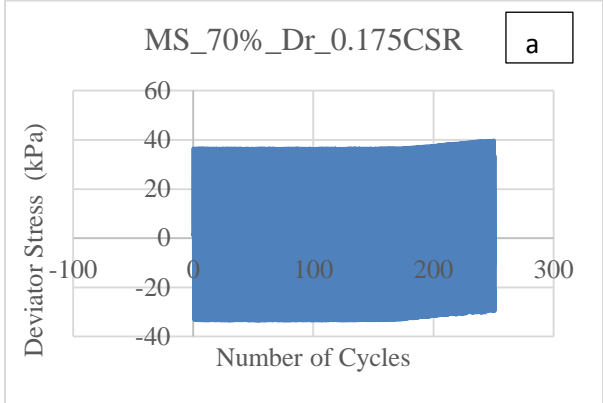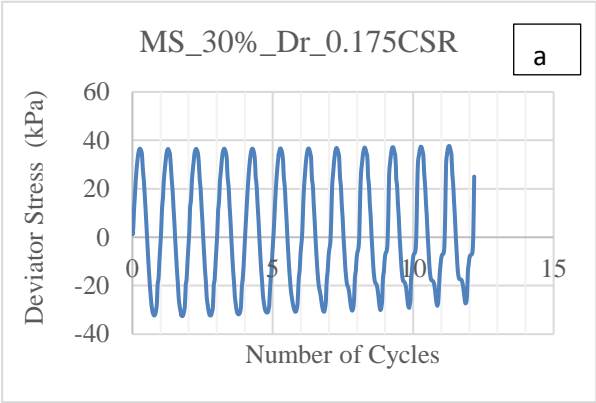
Figure 5. Cyclic triaxial test of 30 % relative density specimen on clean sand: (a) deviator stress vs. number of cycles (b) axial strain vs. number of cycles (c) excess pore water pressure vs. number of cycles

Figure 6. Cyclic triaxial test of 70 % relative density specimen on clean sand: (a) deviator stress vs. number of cycles (b) axial strain vs. number of cycles (c) excess pore water pressure vs. number of cycles
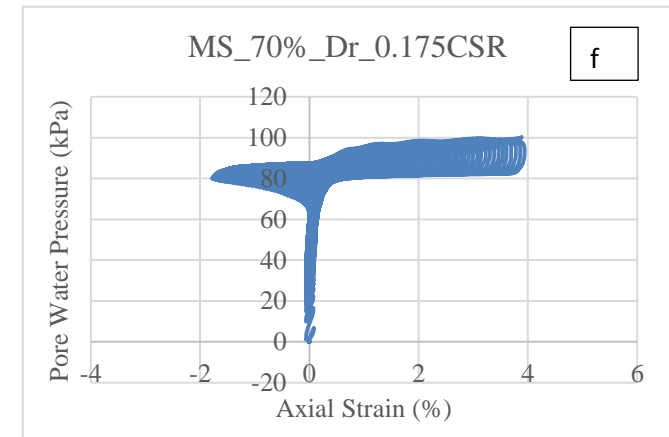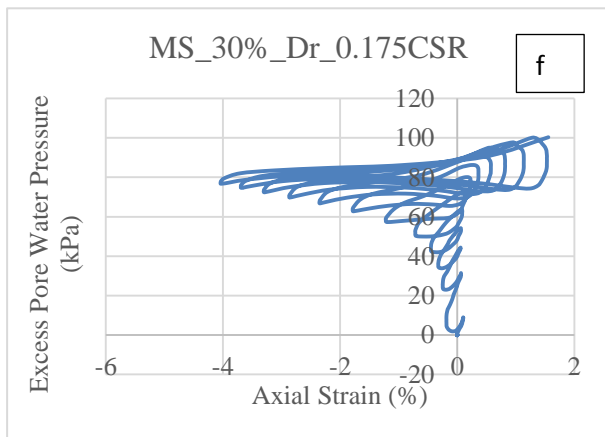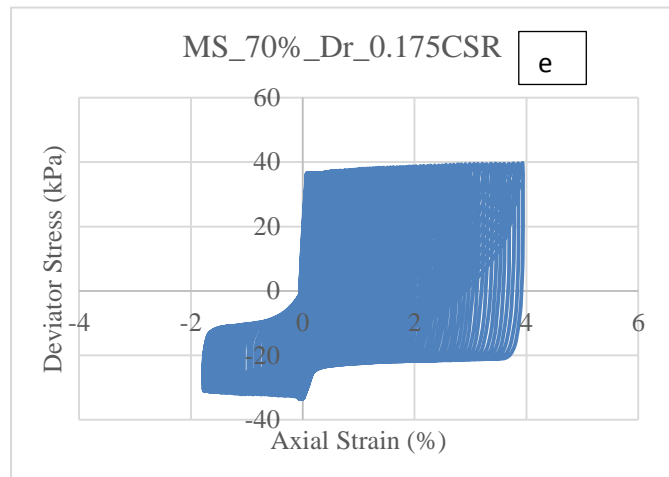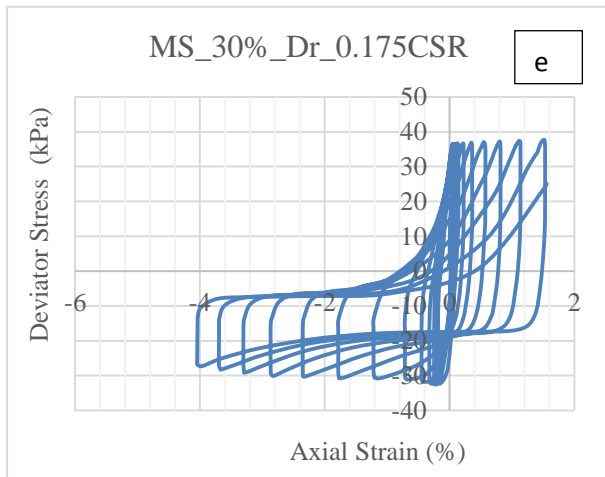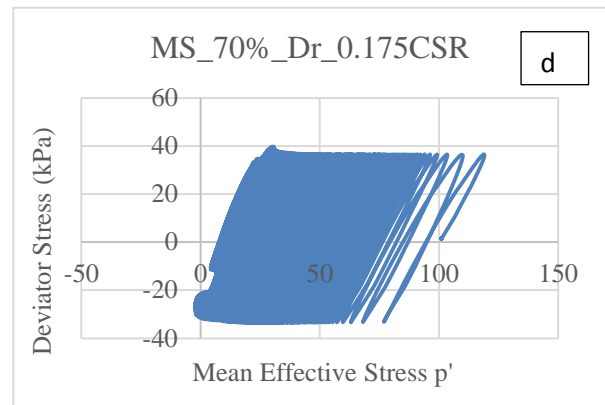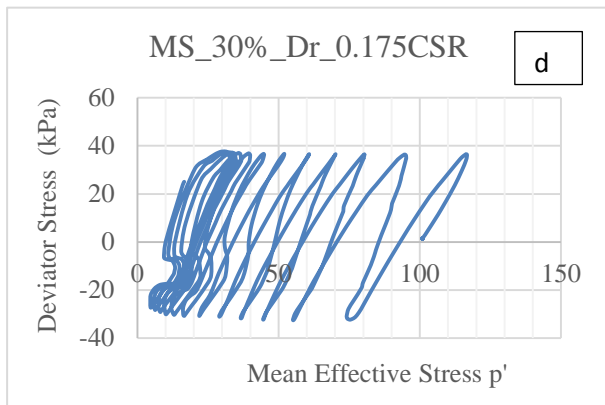
Figure 5. Cyclic triaxial test of 30 % relative density specimen on clean sand: (d) Effective stress-path (e) stress-strain curve (f) strain path of loose sand

Figure 6. Cyclic triaxial test of 70 % relative density specimen on clean sand: (d) Effective stress-path (e) stress-strain curve (f) strain path of loose sand

The effective stress path (deviator stress vs. mean effective stress) obtained from the same test corresponding to the 30 % & 70 % relative density is shown in Figure 5 (d) & 6 (d). It can be seen in

both cases that the effective stress path is shifted from the extreme right to the extreme left position (approaches to zero from 100 kPa). The first arrival of the stress-path to the extreme left position (zero) is called the state of initial liquefaction or onset of initial liquefaction (Kramer 1996). At this point, soil loses its shear strength completely (effective stress is zero) as the soil loses its grain-to-grain contacts between them due to the increase in pore water pressure and rapid increase in the strain amplitude as shown in Figure 5 (b) & 6 (b).

Figures 5 (e) & 6 (e) illustrates the stress-strain behaviour of the same test specimen obtained from 30 % & 70 % relative density sample. It can be observed from Figure 5 (e) that the effective stress decreases and amplitude of strain increase with the progressive number of cycles. It is also clear that the secant shear modulus tends to decrease while strain range tends to widen with the increase in the number of cycles. The same can be observed for the dense specimen (Figure 6e), however, in the dense case, unlike loose specimen, widening of the strain range occurs with low mobilized shear resistance with each progressive number of cycles. This increase of shear resistance at some strain with the increase in the number of cycles is due to the positive dilatancy of the soil skeleton, which is referred as "cyclic mobility" (Kramer 1996). The dilative nature of the dense sand prevents the large development of the shear strain amplitude; on the contrary, loose sand undergoes large shear strain development due to the contractive nature (negative dilatancy) of the soil skeleton. Hence, it is obvious that dense and compacted sand would have greater resistance to liquefaction than those of loose sand. Similar results were reported by (Ha et al. 2011) in the literature.

The relationship between the development of excess pore water pressure and axial strain amplitude is shown in Figure 5 (f) & 6 (f). Figure 5 (f) depicts the behaviour of the loose sand specimen and Figure 6 (f) depicts the behaviour of dense sand specimen corresponding to the same test results as discussed above. It can be noted from Figure 5 (f) that and loose sand specimen becomes extremely soft and quickly develops the large strain amplitude when the excess pore water pressure build-up exceeds 60 % of the initial consolidation stress. Nonetheless, dense specimen exhibits somewhat better resistance against the development of the large shear strain amplitude and pore water pressure development (Figure 6f).

Re-liquefaction potential of dense and loose sand

The liquefaction and re-liquefaction potential of Manu riverbed sand obtained from the test specimen corresponding to 70 % relative density and Cyclic Stress Ratio of (CSR) of 0.20 is shown in Figure 7. The horizontal axis represents the development of the axial strain amplitude and the vertical axis represents the development of the excess pore water pressure to cause initial liquefaction. As discussed earlier, in each case the liquefaction test is stopped when the double amplitude axial strain reached 5 % or excess pore water pressure developed is equal to the effective consolidation pressure (100 kPa) and subsequent reliquefication test is followed. Figure 7 (a) illustrates the first liquefaction test result of the densely packed specimen followed by 2nd, 3rd, 4th liquefaction test (re-liquefaction) on the same specimen and illustrated in Figure 7 (b), 7 (c), 7 (d). The number of cycles required to cause initial liquefaction and re-liquefaction is summarized in Table 2.

Table 2. Summary of number of cycles required to cause initial liquefaction and re-liquefaction

Relative Density	Test Number	NL (Cycles)	CSR
70%	1st Liquefaction	102	0.20
78%	2nd Liquefaction	70	0.20
82%	3rd Liquefaction	193	0.20
88%	4th Liquefaction	395	0.20

*NL= Number of cycles to cause initial liquefaction, CSR= Cyclic stress ratio

It has been found that (as given in Table 1) despite an increase in the relative density after the first liquefaction test, the second liquefaction (re-liquefaction) resistance is decreased significantly i.e., re-liquefaction (second liquefaction) occurs at a smaller number of cycles (NL = 70 cycles) than the first

liquefaction (NL = 102 cycles). However, the third and fourth liquefaction resistance shows greater than the previous liquefaction resistance. This is in accordance with the results of Oda et al. (2001), Ha et al. (2011). The relative density of the soil specimen increases in each test as the re-consolidation (expulsion of excess pore water) is allowed to occur for about 20 minutes following the post-liquefaction test. The same trend is observed for 30 % relative density specimen tested at 0.20 CSR.

Figure 7 (a) (first liquefaction test) indicates a gradual increase in the development of the excess pore water pressure and uniform increase of the strain amplitude up to 60 % of the effective consolidation stress, after which sudden increase in the strain amplitude with the increase in the number of cycles is observed. However, the same is not true for 2nd, 3rd, and 4th liquefaction test. It can be observed in Figure 7 (b), 7 (c), & 7 (d) that after the first liquefaction test the development of the excess pore water pressure (for 2nd, 3rd, 4th liquefaction test) was so rapid that it rises to more than 60 % of the effective consolidation stress in less than a cycle. Simultaneously, the sudden development of large strain amplitude (greater than 1 %) can be noticed in less than a cycle.
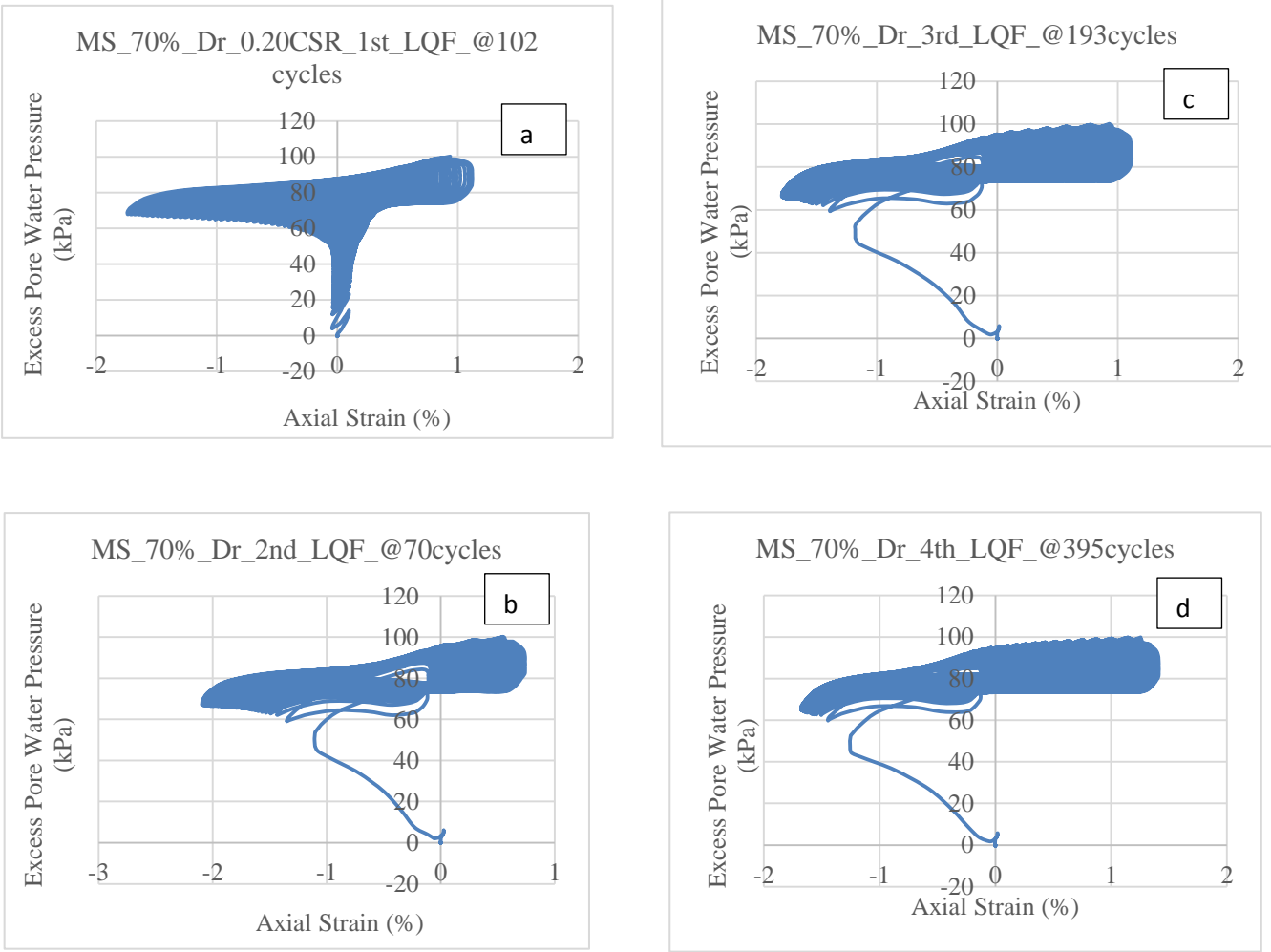
Figure 7. Cyclic triaxial test of 70 % relative density specimen on clean sand: (a) First liquefaction (b) 2nd liquefaction (c) 3rd liquefaction (d) 4th liquefaction

Thus, it can be concluded that re-liquefaction can occur in both loose and densely packed specimen of the tested Manu riverbed sand (clean sand). It was reported in the previous investigation by Xenaki & Athanasopoulos (2003) that the liquefaction resistance of the sand-silt mixtures is found to be less

compared to those of clean sand up to some limiting fines content. During 3 January 2017 Tripura earthquake sand containing an appreciable percentage of silt was ejected to the ground surface. Hence, in future the same Manu river sand would be mixed with different percentage of fines and investigations on liquefaction and re-liquefaction potential of the sand-silt mixtures will be done and will be reported elsewhere.

CONCLUSIONS

The laboratory and in-situ site investigation of the liquefaction site caused due to 3 January 2017 Tripura earthquake, India, yields the following conclusions.

- The possible in-situ liquefaction zone based on the Multichannel Analysis of Surface Wave (MASW) test was observed to be at depths less than 7 m below the ground surface. The outcomes of this study may serve as additional data and unlock several future scopes in the understanding of the geotechnical earthquake engineering of the region.
- The dilative nature of the dense sand (cyclic mobility) prevents the large development of the shear strain amplitude during cyclic loading. Thus, the loosely prepared sand specimen is more likely to liquefy in a smaller number of cycles than the densely prepared specimen.
- The re-liquefaction potential (for the 2nd time) of the sand reduced significantly than the first liquefaction resistance. However, subsequent 3rd and 4th liquefaction resistance is greater than the 2nd time liquefaction due to rearrangement of the sand particles during reconsolidation and cyclic loading.
- The test results demonstrated that the re-liquefaction susceptibility of the Manu riverbed sand does exist. Hence, it may be inferred that the same site can re-liquefy in future earthquake events of magnitude more than 6.

ACKNOWLEDGEMENT

REFERENCES

Anbazhagan, P., Mog, K., Rao, K.N., Prabhu, N.S., Agarwal, A., Reddy, G.R., Ghosh, S., Deb, M.K., Baruah, S. and Das, S.K., 2019. Reconnaissance report on geotechnical effects and structural damage caused by the 3 January 2017 Tripura earthquake, India. *Natural Hazards*, pp.1-26.

ASTM, D., 2013. Standard test method for load controlled cyclic triaxial strength of soil. *Annual Book of ASTM*, *11*.

Chandran, D. and Anbazhagan, P., 2017. Subsurface profiling using integrated geophysical methods for 2D site response analysis in Bangalore city, India: a new approach. Journal of Geophysics and Engineering, 14(5), pp.1300-1314.

Ha, I.S., Olson, S.M., Seo, M.W. and Kim, M.M., 2011. Evaluation of reliquefaction resistance using shaking table tests. *Soil dynamics and earthquake engineering*, *31*(4), pp.682-691.

Huang, Y. and Yu, M., 2013. Review of soil liquefaction characteristics during major earthquakes of the twenty-first century. *Natural hazards*, *65*(3), pp.2375-2384.

Indian Standard, I.S., 2016. Criteria for earthquake resistant design of structures. *5th Revision, Bureau of Indian Standards, New Delhi, India*.

Kramer, S., 2005. L. (1996). Geotechnical Earthquake Engineering. *Pren-tice Hall, New Jersey*.

Mog, K. and Anbazhagan, P., 2018, November. Dynamic Properties of Surface Liquefied Site Silty-Sand of Tripura, India. In *International Congress and Exhibition" Sustainable Civil Infrastructures: Innovative Infrastructure Geotechnology"*(pp. 140-154). Springer, Cham.

Oda, M., Kawamoto, K., Suzuki, K., Fujimori, H. and Sato, M., 2001. Microstructural interpretation on reliquefaction of saturated granular soils under cyclic loading. *Journal of Geotechnical and Geoenvironmental Engineering*, *127*(5), pp.416-423.

Sitharam, T.G., Govindaraju, L. and Murthy, B.S., 2004. Evaluation of liquefaction potential and dynamic properties of silty sand using cyclic triaxial testing. *Geotechnical Testing Journal*, *27*(5), pp.423-429.

Tokimatsu, K., KUWAYAMA, S., Tamura, S. and MIYADERA, Y., 1991. Vs Determination from steady state Rayleigh wave method. *Soils and Foundations*, *31*(2), pp.153-163.

Tokimatsu, K., Tamura, S. and Kojima, H., 1992. Effects of multiple modes on Rayleigh wave dispersion characteristics. *Journal of geotechnical engineering*, *118*(10), pp.1529-1543.

Towhata, I., 2008. *Geotechnical earthquake engineering*. Springer Science & Business Media.

Xenaki, V.C. and Athanasopoulos, G.A., 2003. Liquefaction resistance of sand–silt mixtures: an experimental investigation of the effect of fines. Soil Dynamics and Earthquake Engineering, 23(3), pp.1-12.